

# Dynamic Referencing in 3D Optical Metrology for Higher Accuracy in Shop Floor Conditions

**Jean-François Larue<sup>1</sup>**

Product Director

Creaform France

[jflarue@creaform3d.com](mailto:jflarue@creaform3d.com)

**Marc Viala, Ph.D.<sup>1</sup>**

R & D Director Creaform

France

[mviaia@creaform3d.com](mailto:mviaia@creaform3d.com)

**Daniel Brown<sup>2</sup>**

Product Manager

Creaform Inc.

[dbrown@creaform3d.com](mailto:dbrown@creaform3d.com)

**Charles Mony, Ph.D.<sup>2</sup>**

Chief Technological

Officer

Creaform Inc.

[cmoney@creaform3D.com](mailto:cmoney@creaform3D.com)

<sup>1</sup> Creaform France - 24 rue Jean-Pierre Timbaud - 38600 Fontaine - France

<sup>2</sup> Creaform head office— 5825 rue St-Georges, Lévis, Québec, Canada G6V 4L2

Word

Count:

5259

Number of Images Submitted: 16

## Abstract

*This paper describes the principles of dynamic referencing for optical CMMs and demonstrates the advantages of this new functionality in terms of measurement accuracy in shop floor conditions. Recent optical triangulation-based CMMs are now able to simultaneously measure multiple 3D points. With the help of markers placed on the part being measured, it is now possible to continuously monitor any deviations from the reference part. In this way, the machine reference and part reference become one and the same and remain locked on the part throughout the measuring process. This significantly improves the accuracy of portable CMMs operating in challenging shop floor environments that are subject to intense vibrations, thus eliminating the need to acquire expensive heavy equipment to ensure measurement accuracy. This article describes the vibration conditions common in factory environments as well as the experiments we designed to reproduce these disturbances and assess their impact on measurement processes using a portable CMM. We conclude with examples from real-life situations.*

## 1. Introduction

Over the past 30 years, one of the most important changes in metrology has been the development of portable measuring devices. This has brought inspection right into the production line, as close to the part as possible. The change—sparked by the development of portable measuring arms in the early 1990s and the emergence of laser trackers shortly after—turned conventional industry inspection methods completely upside down. It also made it possible to take measurements more quickly and more often, fostering huge improvements in response time and quality.

Far from the comfort of metrology labs where qualified inspectors operate digital CMM with their heavy, stable granite table, portable measurement is still facing several major challenges. In production environments, permanent vibrations generated by production equipment (e.g., machining centers, presses, carriage equipment, cranes), the requirement for rigid equipment setups, changes in temperature and humidity levels, and operators' varying experience and skills levels are the daily obstacles faced by users of portable measurement solutions.

Optical solutions introduce innovative concepts like self-positioning or dynamic referencing, which enables the measuring device to be continuously locked to the part by an optical link. The purpose of this article is to evaluate the contribution of these new technologies in quality control operations in shop floor conditions.

After analyzing the measuring process in real shop floor conditions, we will analyze the impact of vibrations on the measurement process and loss of accuracy. This analysis is supported in part by a presentation of the vibration levels prevailing in generic plants. Then, we analyze the impact of such vibrations on the measuring device using an experimental setup reproducing “shop floor-like” conditions and standards for accuracy evaluation like ASME B89.4.22 [1].

The article describes the theoretical principles implemented to guarantee the dynamic referencing of an optical measuring device relative to the part or equipment to be measured. It also presents the results of an experimental plan implementing simulated vibrations conditions that are close to the actual conditions in a production plant. Under such simulated conditions, an accuracy evaluation is made using a standard gage.

Another experiment using a CMM as a reference mean shows that a very high degree of accuracy can be achieved despite unstable measurement conditions.

Lastly, we present some results showing how automatic alignment and dynamic referencing features can positively impact the behavior of coordinate metrologists and reduce the risk of poor measurement. This part is based on some methodologies extracted from the report “How Behavior Impacts Your Measurement,” issued by CMSC in 2011.

We conclude this contribution with real cases from the aerospace industry. These applications will allow us to better understand the advantages of the dynamic referencing and self-positioning concept.

## 2. **Vibration conditions in the factory environment**

- **Vibration sources**

There are numerous sources of vibration in a production or shop floor environment, including

- Nearby road and rail traffic
- Production equipment (presses, machining centers)
- Handling equipment (e.g., forklifts, gantry cranes)
- Operators

If the shop floor is inadequately insulated against vibration, these vibrations are subsequently transmitted to the measuring system and the object being measured, and may even be amplified if an unstable tripod or nonrigid base is being used.

- **Vibration levels**

Specific standards exist to define methods for quantifying factory vibrations (notably due to their potential impact on human health). We will refer to ISO 2631.2–2003 [2] and ANSI S3.29–1983 [3]. It is widely recognized that the most prevalent factory vibration levels—and the ones most likely to cause disturbances—are those ranging from 1 Hz to 80 Hz (higher frequencies are partially filtered by cement floors). Vibrations are often quantified in terms of velocity and acceleration. Most standards establish a health risk threshold of 0.64 m/s<sup>2</sup> (effective value) on the vertical axis for 8 hours of daily exposure. The ISO 2631 standard establishes the acceptable threshold for workers at 0.04 m/s<sup>2</sup> (weighted effective value).

Various studies have helped characterize acceptable levels of continuous vibration. For example, Australia’s Department of Environment and Conservation [4] establishes acceptable levels for different locations, as shown in the table below. They include the 0.04 m/s<sup>2</sup> value recommended in the ISO 2631 standard for workshops (continuous vibration). Note, however, that impulsive vibration values can be as high as 1.28 m/s<sup>2</sup>.

Location	Assessment period	Preferred values		Maximum values	
		z-axis	x- and y-axes	z-axis	x- and y-axes
<b>Continuous vibration</b>					
Critical areas	Day- or night-time	0.0050	0.0036	0.010	0.0072
Residences	Daytime	0.010	0.0071	0.020	0.014
	Night-time	0.007	0.005	0.014	0.010
Offices, schools, educational institutions and places of worship	Day- or night-time	0.020	0.014	0.040	0.028
Workshops	Day- or night-time	0.04	0.029	0.080	0.058
<b>Impulsive vibration</b>					
Critical areas	Day- or night-time	0.0050	0.0036	0.010	0.0072
Residences	Daytime	0.30	0.21	0.60	0.42
	Night-time	0.10	0.071	0.20	0.14
Offices, schools, educational institutions and places of worship	Day- or night-time	0.64	0.46	1.28	0.92
Workshops	Day- or night-time	0.64	0.46	1.28	0.92

Table 1: Preferred and maximum weighted RMS values for continuous and impulsive vibration acceleration ( $m/s^2$ ) 1-80 Hz [4]

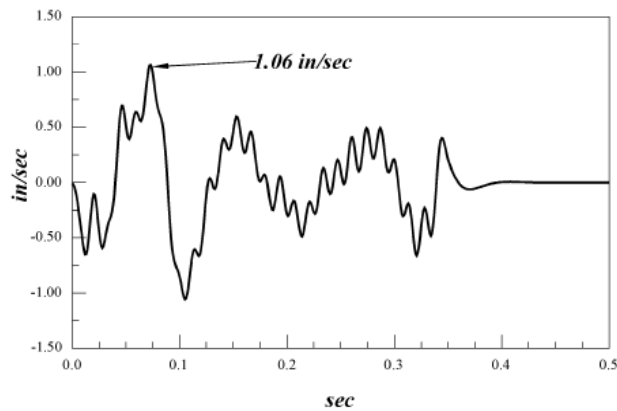


Table 2: Predictions of press-induced soil vibrations (instant velocity as a function of time) at a projected CMM location

Another study [5] presents examples of vibrations recorded in an urban environment (city of Montreal) and representing disturbances generated by heavy vehicles (buses and trucks). In buildings near roadways, traffic can generate vibrations with point acceleration levels between 0.005 and 2  $m/s^2$  and velocities between 0.05 and 25 mm/s for frequencies ranging from 5 to 25 Hz.

To conclude this section, a further study [6] presents vibrations recorded directly on site at production facilities. This study, which was conducted prior to installation of a CMM in a factory operating stamping presses, found vibrations of up to 1.06 in./sec (26.9 mm/s) with a typical frequency of 17 Hz (soil resonance frequency) at a distance of 50 ft. from the press.

One final study [7] carried out in France by INRS (National Research and Safety Institute), also presents several noteworthy values recorded near industrial machines:

- Smelter molding press: 0.2 to 0.5  $m/s^2$  between 3.6 and 9 Hz
- Stamping press: 0.25 to 1.15  $m/s^2$
- Drop hammer: 2 to 60  $m/s^2$

These studies show that accelerations of up to 2  $m/s^2$  and velocities of up to 25 mm/s for impulsive vibrations are extreme values that can be expected in a shop environment. Acceleration values of 0.2  $m/s^2$  and velocities of 2.5 mm/s are, for their part, commonplace in any work environment. It was this level of vibration that we subsequently sought to reproduce at the experimental level.

- **Experimental setup**

To reproduce vibrations experimentally, we used an ABB IRB 4400 robot arm programmed to execute small amplitude up-and-down movements (instruction: 1.5 mm) as rapidly as possible. These were at the limit of servo-control capabilities for the robot arm.

Displacement was measured using an optical tracking solution.

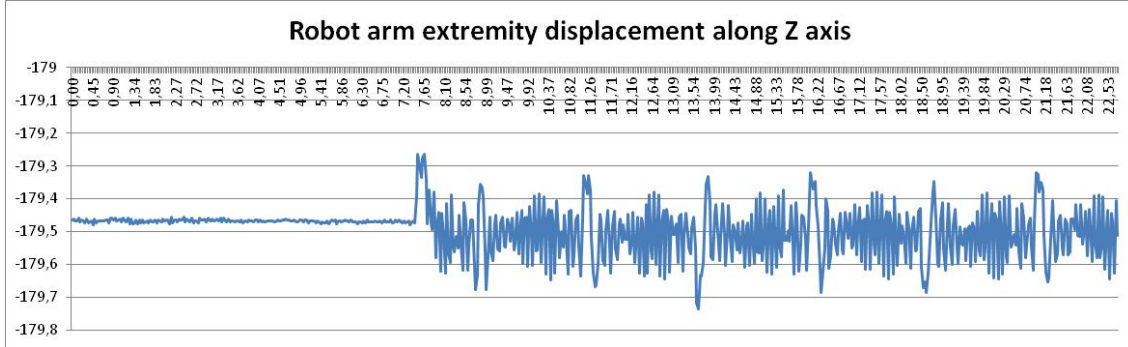


Table 3: *Vibration amplitude measured at end of robot arm (Vertical displacement in mm as a function of time in seconds)*

In the end, we observed displacement with a maximum crest-to-crest amplitude of 0.4 mm. Frequency analysis of the displacement showed a main frequency in the 10 Hz range, whereas we observed effective accelerations in the order of  $0.25 \text{ m/s}^2$ . Velocities obtained were in the order of 3.4 mm/s (average quadratic error). These results were very close to the objective we had set.

### 3. Dynamic referencing

- **Optical CMMs**

Optical CMMs using image-based triangulation are constituted of an optical tracking system equipped with video cameras. There are two categories of optical CMMs: those based on matrix array cameras (which use retro-reflective targets or LEDs as targets) and those with linear array cameras (which systematically use LEDs as targets). This paper deals only with the first category.

Optical CMMs use three main calculation steps to implement their dynamic referencing and optical measurement functionalities:

- An image processing step to accurately assess target image projections in the stereo sensor images
- A triangulation step to estimate the target coordinates  $(X, Y, Z)$  in the sensor reference from their projections in the twin images of the stereo sensor
- A step to estimate the pose of a modeled object using a set of points whose nominal coordinates are known and observed by stereo sensor

The cameras can be modeled using perspective projections and other parameters that take into account geometric aberrations generated by the imager (camera with its lens), commonly known as radial and tangential distortions. Identification of these so-called intrinsic parameters occurs during a previous calibration step. The approach used to calibrate the imagers is based on techniques used in photogrammetry (Atkinson 1996).

With this calibration, the projection of a 3D point  $\mathcal{P}$  expressed in the stereo sensor reference in one of the imagers is given by the following perspective projection relationship (Faugeras 1993; Hartley et al. 2004):

$$\mathbf{x} = \mathbf{P} \mathbf{X} \quad (1)$$

Where  $\mathbf{X} = (X, Y, Z, 1)^t$  represents the homogenous coordinates of  $\mathcal{P}$ ;  $\mathbf{x} = (u, v, 1)^t$  the coordinates of the projection; and  $\mathbf{P}$  the projection matrix:

$$\mathbf{P} = \begin{pmatrix} \mathbf{P}_1 \\ \mathbf{P}_2 \\ \mathbf{P}_3 \end{pmatrix} = \mathbf{K} \times \left( \begin{array}{c|c} \mathbf{R} & \mathbf{t} \\ \mathbf{0}_{1 \times 3} & 1 \end{array} \right) \quad (2)$$

$\mathbf{K}$  being the camera matrix integrating only its intrinsic parameters (we ignore here the additional radial and tangential distortion correction parameters):

$$\mathbf{K} = \begin{pmatrix} A_u & 0 & C_u \\ 0 & A_v & C_v \\ 0 & 0 & 1 \end{pmatrix} \quad (3)$$

And where  $\mathbf{R}$  and  $\mathbf{t}$  represent the rigid transformation (rotation matrix  $\mathbf{R}$  and translation vector  $\mathbf{t}$ ) ensuring the transfer from the sensor reference frame to the imager reference frame.

This relationship is the basis for calculating the coordinates of point  $\mathcal{P}$  by triangulation and for calculating the pose of an object.

The image processing step consists of extracting the images acquired by the stereo sensor, i.e., the target center projections observed in the sensor environment. This step significantly influences optical sensor performance, both in terms of repeatability and accuracy.

Several approaches are documented in the literature (Shortis et al. 1994; Shortis et al. 1995; Otepka 2004). Some involve calculating the grayscale barycenter of the target light response, while others involve approximating the response curves by ellipses or modeling the responses. In the latter cases, estimation of the model is based on a least-squares estimator between the pixel value in image  $I$  and the pixel value determined by the model  $\hat{I}(\mathbf{p}_{model})$ :

$$C_{min}(\mathbf{p}_{model}) = \sum (\hat{I}(\mathbf{p}_{model}) - I)^2 \quad (4)$$

The photogrammetric step after subpixel target detection is triangulation; in this step, the traces of a target captured in the two stereo sensor images are measured and used to calculate the target coordinates  $(X, Y, Z)$  in the sensor reference.

Numerous techniques are available to infer coordinates of a target from its projections in a pair of stereo images (Atkinson 1996; Hartley et al. 1997). The simplest is to calculate the midpoint. Geometrically, this solution consists of taking the midpoint of the common perpendicular joining the two optical rays running through the traces and the target (cf. Figure 1).

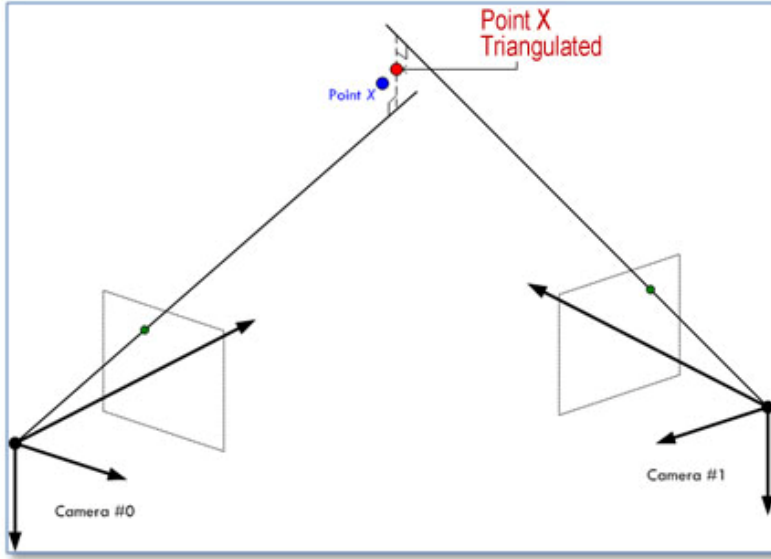


Figure 1: Principle of midpoint triangulation

Other approaches involve solving a linear system using perspective projection relations (1) or (2) solving a polynomial equation (Hartley et al., 1997).

Once target triangulation is complete, targets are identified as belonging to a rigid body or not: a rigid body can be described as a series of targets rigidly linked in their own reference frame. Identification is followed by 3D localization of the rigid bodies through measurement of their 3D targets and nominal coordinates; 3D localization makes it possible to estimate the position and orientation of the rigid body's reference frame, or pose, in relation to a measurement reference, in this case the sensor reference. Once 3D localization of the rigid body has been estimated, the position of the probe center is deduced.

The 3D localization step is crucial to measurement performance and can be based on a linear localization method that models rigid body orientation using a quaternion (Horn 1987). This method has been shown to be effective in simulations (Eggert et al. 1997).

The other possible technique tackles a 2D/3D calculation problem by drawing not on the coordinates of measured targets, but rather on the targets' projections in the stereo sensor imagers. This technique, known as *resection*, is widely used in photogrammetry (Karara 1989) and has the advantage of minimizing error directly in the target measurement space. In the computer vision literature, this problem is known as the *PnP<sup>l</sup> problem*. In its initial formulation, it is nonlinear if we consider the perspective projection relationship (1), and can be solved by minimizing a criterion in the least squares sense:

$$C_{min}(\hat{\mathbf{R}}, \hat{\mathbf{t}}) = \sum_{i=0}^N \left\| \begin{pmatrix} {}^0\mathbf{f}(X_i) - {}^0\mathbf{x}_i \\ {}^1\mathbf{f}(X_i) - {}^1\mathbf{x}_i \end{pmatrix} \right\|^2 \quad (5)$$

Where  $(\hat{\mathbf{R}}, \hat{\mathbf{t}})$  represent the pose rotation and translation parameters to be estimated,  $(X_1, \dots, X_N)$  the nominal coordinates of  $N$  points in the object reference,  $({}^0\mathbf{x}_1, \dots, {}^0\mathbf{x}_N)$ , and  $({}^1\mathbf{x}_1, \dots, {}^1\mathbf{x}_N)$  and the coordinates of their projections in the first imager and stereo sensor, respectively.  ${}^j\mathbf{f}(\dots)$  represents the perspective projection function for  $j$  given by equations (1) and (2); that is to say:

---

<sup>1</sup> For Perspective N-Point.

$${}^j\mathbf{f}(X_i) = \begin{pmatrix} {}^j\mathbf{P}_1(X_i) \\ {}^j\mathbf{P}_2(X_i) \\ {}^j\mathbf{P}_3(X_i) \end{pmatrix} \quad (6)$$

The rigid body concept applies in equal measure to probes and scanners that are identically instrumented with targets and localized in 3D by an optical localization system.

Once the calculation is performed, we can deduce the position of the center of the probe ball at all times (using a prior calibration step to determine the position of the ball center in the reference defined by the probe targets). The same deduction can be made if the tip is replaced by an optical probe using a laser line projection and camera (scanner).

- **Dynamic referencing**

Cameras in an optical localization system can simultaneously observe other targets than those present on the probe. For example, targets can be positioned in advance on the object to be measured. Since these targets are measured at the same time as the probe targets, it is possible to calculate not only the probe position, but the part position at the time a point is probed. Since matrix cameras are used, all targets are also triangulated synchronously at a frequency of 30 Hz (whereas certain optical localizers use linear cameras that can only acquire targets sequentially). This makes it possible to calculate probe position in direct relation to the part, and not just the machine reference. All measuring operations are thus performed directly in the part reference and will not be affected by possible movements—even rapid ones—of either the part or the optical localization system. This functionality is known as dynamic referencing. It is the core of the *TRUaccuracy* technology featured in Creafom products.

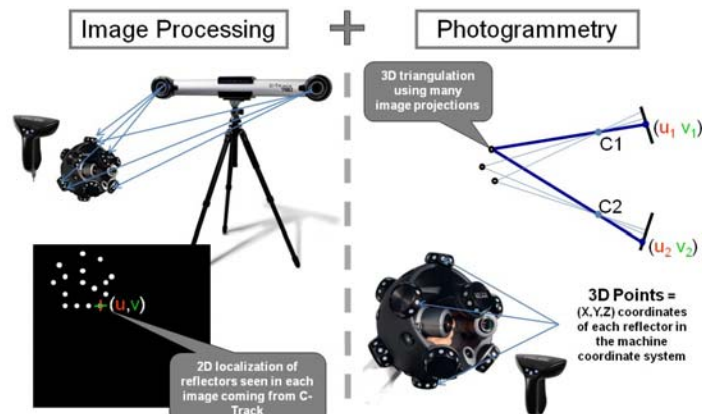


Figure 2: Operating principles of an optical CMM using image-based triangulation



Figure 3: Operating principle of dynamic referencing

Thanks to this technology, optical CMMs can be mounted on a light tripod for unmatched portability (in the case of handheld, self-positioning scanners, the tripod is dispensed with altogether). The operator can thus move freely around the part for easier measurement of hard-to-access points, without any loss of alignment.

Most of all, in a shop environment affected by extensive vibrations, as noted above, dynamic referencing makes it possible to maintain levels of uncertainty normally found only in metrology laboratories. As we shall show below, as a result of dynamic referencing, vibrations have no negative effect on measurement uncertainty.

#### 4. Experimental results

- **First experiment: laboratory evaluation of the impact of vibrations on a portable polyarticulated arm CMM and a portable optical CMM**

The machines tested were an 8 ft. polyarticulated arm and a portable optical CMM.

To experimentally demonstrate dynamic referencing performance, the experimental setup described in Chapter 2 was used. The robot's load characteristics made it possible to attach the portable measurement machine (respectively, the polyarticulated arm and the optical localization system) to the end of the robot arm.

Accuracy tests were conducted using a 2.5 m standard measurement gage fitted with cones, an artifact commonly used for accuracy testing under the VDI 2634 standard [8]. This artifact consists of a high modulus carbon fiber beam with a very low thermal elongation coefficient to which are affixed cones serving as isostatic bases for a spherical probe. The beam is attached to a heavy tripod. Figure 4 shows the artifact on the tripod. The distances between cones were calibrated with a diameter sphere comparable to the probe spheres used to minimize calibration error. Calibration uncertainty for the distances is  $1.5 \mu\text{m} + 1 \mu\text{m} \times L$  with an expansion factor of  $k = 2$ , knowing that the greatest distance is 2500 mm.



Figure 4: Verification artifact for VDI 2634 standard on its tripod [8]

To ensure dynamic referencing with the optical CMM, retro-reflective targets were first affixed to the artifact and stand. Twenty-one points were measured on the bar over a distance of 2 m and the distances between consecutive points were compared with the calibrated distance listed on the beam's calibration certificate. This gives a measurement error for each of the distances considered (20 distances). Several sets of measurements were taken, the first two without vibrations (robot with brakes applied), the second two with the vibrations described earlier (robot in operation).

The curves below show the results obtained with the two measurement methods studied.

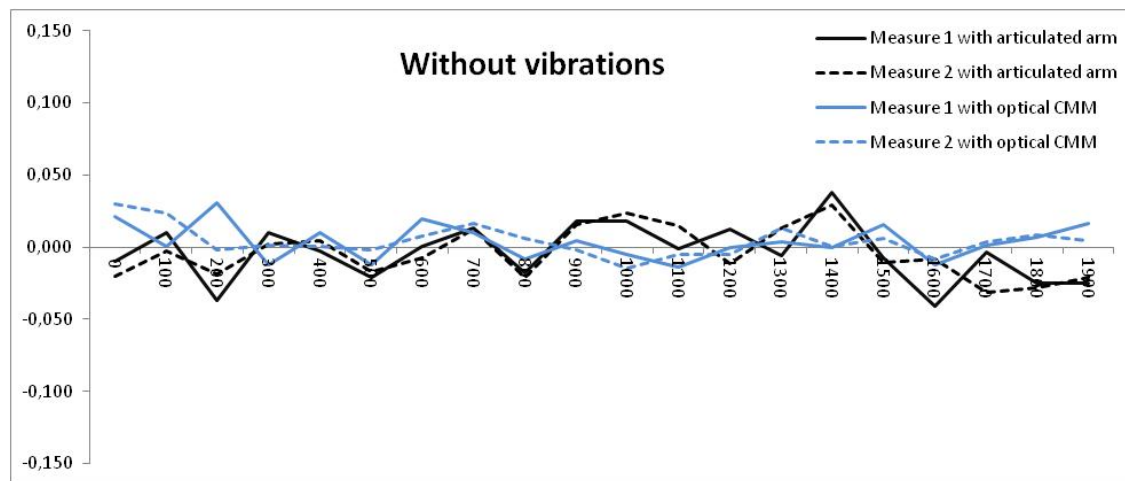


Figure 5: Results of tests without vibrations for each method tested (2 tests each). On the ordinate axis, the deviation between the calibrated and measured value for each of the 20 interdistances.

Without vibrations, the results obtained for both methods were similar, with an average quadratic error (RMS) of 0.018 mm for the arm and 0.011 for the optical CMM. Maximum errors were 0.041 mm for the arm and 0.031 mm for the optical CMM.

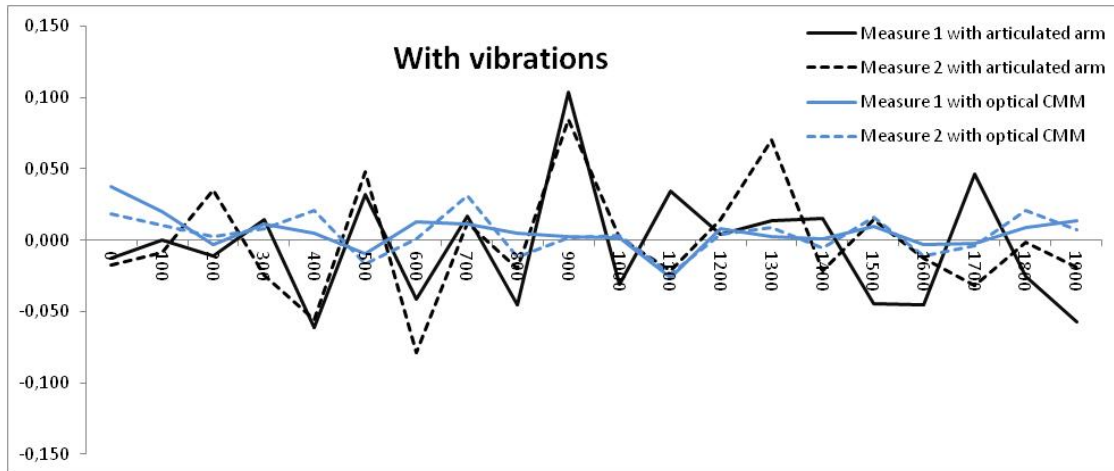


Figure 6: Results of tests with vibrations for each method tested (2 tests each). On the ordinate axis, the deviation between the calibrated and measured value for each of the 20 interdistances.

The results of the tests with vibrations clearly show the advantage of dynamic referencing, with an average quadratic error of 0.039 mm for the arm and 0.013 for the optical CMM. Maximum errors were as high as 0.103 mm for the arm, but did not exceed 0.037 for the optical CMM. There was no notable degradation in optical CMM performance.

The level of vibration simulated is very common in workshop environments. This experiment clearly demonstrated the loss of accuracy experienced with a non-optical portable solution in the absence of a granite table equipped with anti-vibration pads.

- **Second experiment: impact of soil stability on a laser tracker measurement**

This experiment was originally conducted to demonstrate the accuracy levels achievable with the HandyPROBE optical CMM for a part positioning application used in the assembly of Ariane 5 rocket engines. The goal was to achieve an accuracy level of 20 microns in the course of continuous movement over several hundred millimeters.

This experiment showed ground deformation occurring during movement of a gantry CMM and demonstrated the benefits of dynamic referencing.

A setup for translating a reference object was affixed to the granite table of a CMM (Figure 7). The reference object was equipped with a laser tracker SMR. It was also instrumented with retro-reflective targets. The object was in continuous motion between multiple levels. While in motion, it was continuously monitored by the laser tracker and optical CMM. At each level, an object position measurement was also taken by the CMM.



Figure 7: Experimental setup simulating slow movement on a vertical axis

The first trials generated the following results (Figure 8):

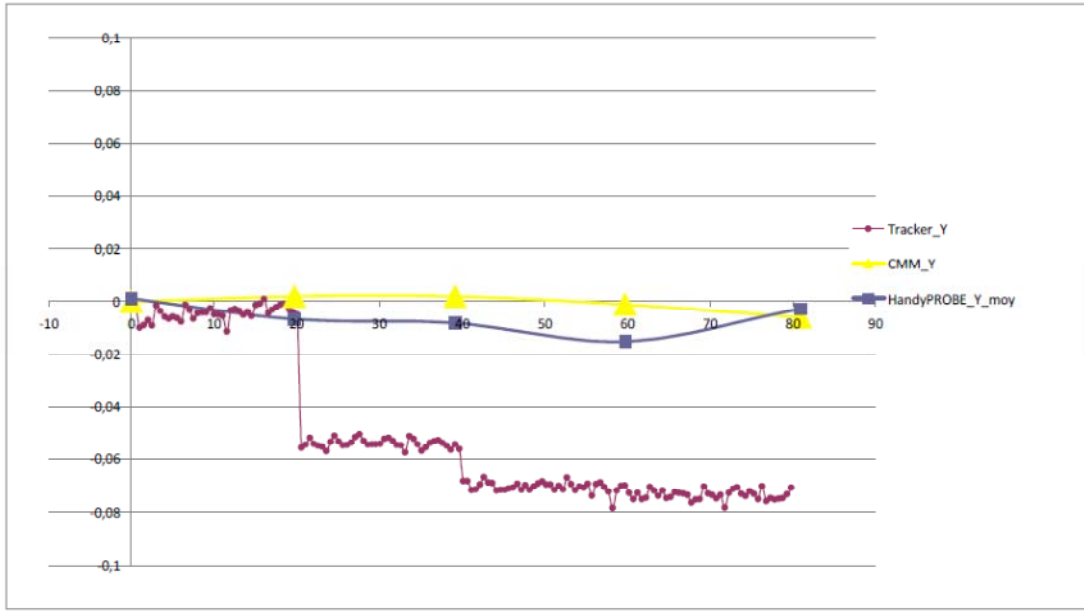


Figure 8: Comparison of laser tracker, CMM and optical CMM measurements along the Y axis (depth). On the abscissa axis, displacement (in mm) and on the ordinate axis, straightness error measured along displacement Y (in mm).

We observe surprising results along the Y axis (depth) for the laser tracker measurements. For each measurement performed with the CMM, we recorded jumps of up to 0.06 mm. Analysis revealed that the CMM's heavy granite table induced imperceptible levels of ground deformation every time the gantry moved. The laser tracker set up on the ground beside the optical CMM was affected by these ground micro-movements, whereas the optical CMM, which used the targets affixed directly to the CMM table as references, was not. In the case of the laser tracker, the error was amplified by the leverage effect: for example, a movement of 10 microns beneath one of the laser tracker's tripod feet will generate an error of 100 microns at a distance of 5 m for a tripod with a radius of 0.5 m. Such ground deformations are common in production workshops and very difficult to detect, which can result in numerous inconsistent measurements.

To confirm the test results, we decided to place the laser tracker directly on the CMM table. The results obtained with this configuration were entirely satisfactory, as shown in the curve below (Figure 9):

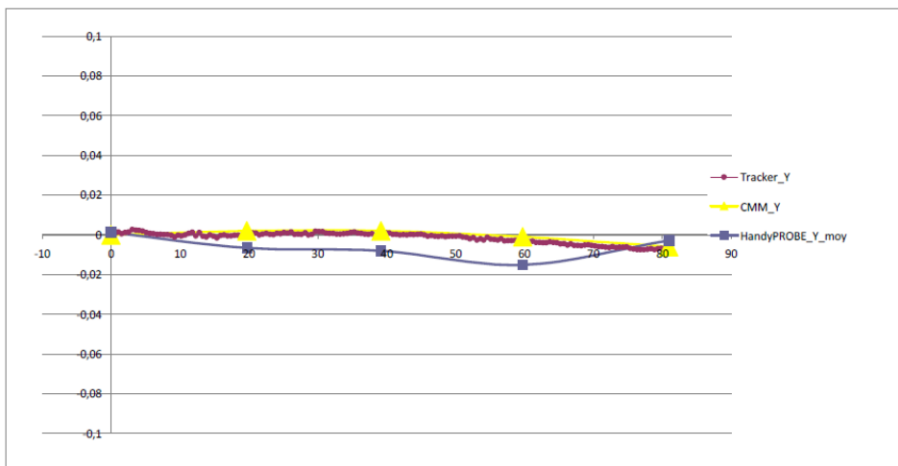


Figure 9: Comparison of laser tracker, CMM and optical CMM measurements with the laser tracker affixed on the CMM table, along the Y axis (depth). On the abscissa axis, displacement (in mm) and on the ordinate axis, straightness error measured along displacement Y (in mm).

In the preceding experiment, differences between the laser tracker and CMM measurements were as great as 80 microns; once placed on the CMM table, however, the laser tracker generated values consistent with the CMM measurements, with deviations of less than 5 microns.

As for the self-positioning HandyPROBE optical CMM, it operated within the 20 micron range as per its specifications. The errors of nearly 1/10 mm observed with the laser tracker were completely eliminated with the optical CMM, thanks to *TRUaccuracy* technology.

This experiment showed that even with a supposedly stable setup (e.g., metrology lab, granite table, heavy base), unexpected movement can occur and seriously affect the uncertainty of measurements performed with a laser tracker-type portable device.

Only *TRUaccuracy* dynamic referencing can guarantee the control of measurement uncertainties of this type.

## 5. Impact on the reduction of operator-related errors

CMSC's 2011 Measurement Study Report entitled "How Behavior Impacts Your Measurement" [19] includes a compelling and detailed analysis of operator behavior in the metrology process.

More specifically, the study indicates that only 6% of participants in the "Day 1: Articulated Arm/Engine Compartment" test noted that the measurement device was on a carpet.

In the "Day 1: Laser Tracker/Door" test, only 6% paid attention to the stability of the part. In this same test, analysis showed that 7% of participants moved the part after aligning, and that only 7% checked drift on one alignment point at the end of measurement.

In the "Day 1: Laser Tracker/Vehicle" test, 20% expressed concerns about the presence of the carpet, 15% questioned part stability, and only 25% mentioned the need to obtain a good alignment.

On the first day of testing, no instructions or procedures were given to participants. Yet more than 40% of the participants worked in the quality control or inspection field and over 60% had at least 7 years of experience and/or performed measurements on a daily or weekly basis.

On the second day, instructions and procedures were provided to the participants. The impact was positive, because 90% of those who took the "Day 2: Articulated Arm/Engine Compartment" test identified the problems posed by the carpet and the large number of people in the measurement area. Nonetheless, less than 30% expressed concern about the stability of the part.

In the Day 2: Laser Tracker/Door test, over 80% of the participants identified the problem with the carpet, but less than 40% expressed concern over the large number of people in the measurement area.

Overall, though, the instructions about measurement quality had a very significant effect, with notable improvements in the deviations observed on day 1 and day 2:

- Engine compartment:      **Day 1:** 0.56 to 3.81 mm.    **Day 2:** 0.15 to 0.90 mm
- Door:                            **Day 1:** 35 to 43.18 mm.    **Day 2:** 0.13 to 0.24 mm
- Vehicle:                        **Day 1:** 5.36 to 8.198 mm.    **Day 2:** 0.926 to 1.59 mm

It is impossible to determine the contribution of errors related to the instability of the measurement setup, but they probably contributed significantly to the errors observed on day 1.

One of the study conclusions is that human error is a major factor in poor quality measurements. Dynamic referencing actively contributes to reducing some of the human errors identified in the CMSC study, i.e., inadequate operator assessment of the risks that derive from an unstable environment, heavy traffic, or an unstable part.

## 6. Sample applications

- **Example 1: Implementation of dynamic referencing to minimize operator error by automating alignment**

Dynamic referencing can also be used effectively to intervene on another parameter identified in the study: alignment quality. Alignment is a key measurement step linking the machine reference to the object reference. With an optical CMM, it is entirely possible, using specialized tools, to position certain targets on points required for alignment. This makes it possible to automatically measure these points and automatically position the optical CMM in relation to the part reference. This eliminates all operator error during the alignment phase and guarantees the best possible alignment, regardless of operator skills. It also minimizes the impact of operator constraints on the measuring tool (pressure on the probe, traction on axis of the arm, etc.)



*Figure 10: Example of a template designed to automate alignment and improve reliability in aeronautical parts measurement*

For example, it is possible to design a tool that immediately places the part in reference without having to measure the least point. The photo in Figure 10 shows a jig developed for the inspection of thrust reverser doors on Airbus engines. Certain targets positioned at precise points (door rotation axis, uplock roller bearing plane) make it possible to automatically align the door.

The fact that the targets are placed at precise points on the jig is another advantage ensuring dynamic referencing and allowing for real-time verification of measurement tool accuracy. Any change in the measured geometry of the optical reference with respect to its reference value makes it impossible to complete the measurement and indicates to the operator that there is a problem with jig deformation or possible measurement drift.

- **Example 2: Implementation of a dynamic positioning model for measuring large parts**

The retro-reflective targets used for dynamic referencing are also compatible with photogrammetry solutions. They make it possible to develop a comprehensive and accurate positioning model using targets affixed to a large object. Once the model is complete, an optical CMM can be placed anywhere that a sufficient number of previously measured targets are visible. In this way, the optical CMM is automatically linked to the global reference. This is particularly useful for measuring large objects.



*Figure 11 : utilisation simultanée de plusieurs équipements dans un environnement particulièrement instable grâce à un modèle de positionnement dynamique construit par photogrammétrie*

For a project with Swiss Jet Aviation AG, one of the world's largest business aviation services companies, Creaform's 3D Engineering Department had the opportunity to measure and digitize the entire interior of a Boeing 737-800.

The goal was to provide Jet Aviation with a detailed representation of the aircraft's as-built fuselage to facilitate custom interior design and outfitting work. Having access to a 3D model would enable company engineers to identify equipment interference risks ahead of time and ensure equipment compatibility with the aircraft's structures and systems right from the start, thereby avoiding long and costly iterations to adjust equipment. Creaform's team of application engineers digitized the entire interior using a combination of handheld Handyscan 3D scanners [20], a long range Leica scanner, several HandyPROBE optical CMMs [21] and MetraSCAN optical CMM 3D scanners [22], and a photogrammetry system [23].

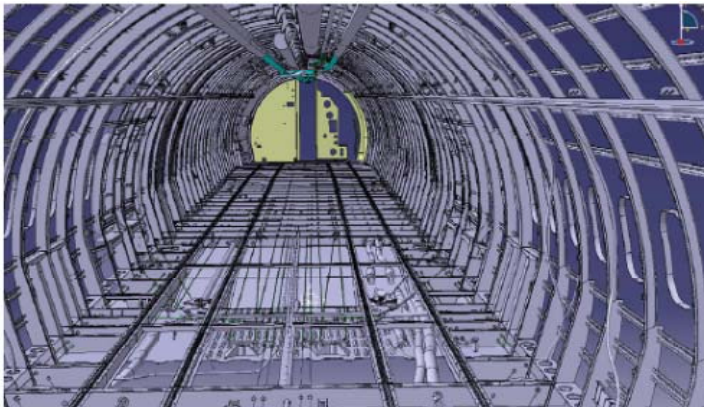


*Figure 12: Reconstructed CAD 3D model of the fuselage*

Once the positioning model had been measured using photogrammetry, it was possible to operate all the equipment simultaneously without realigning the data afterwards, and especially without worrying about vibrations generated by all the activity inside the aircraft. Once data acquisition was complete, the data was processed at Creaform and the model finalized with CATIA.

## **7. Conclusion**

Portable optical CMMs are opening a new chapter in portable 3D measurement. Their capabilities make measurement more reliable, less operator dependent, and more portable than ever. One important benefit of this is to bring measurement directly to the shop environment production line, thereby ensuring greater reactivity during production increases, earlier detection of potential drift, and faster identification of underlying causes.

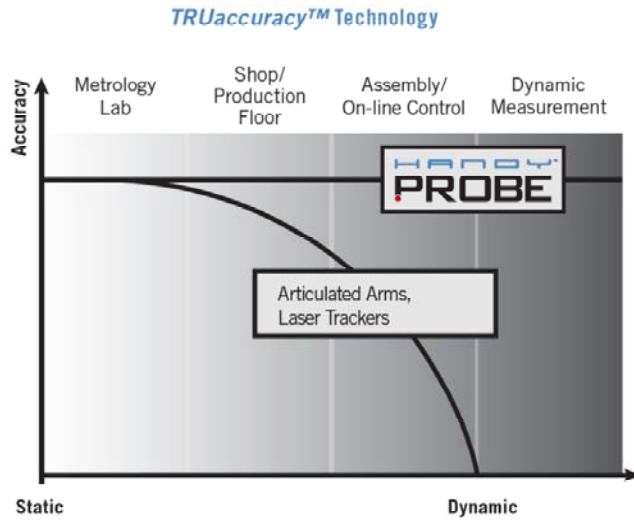


*Figure 13: Degradation of measurement quality with conventional means of measure as a function of environmental stability: from static (perfectly stable and controlled) to dynamic (presence of continuous vibration and movement)*

Creaform's *TRUaccuracy* technology—which includes dynamic referencing, automatic drift detection (through permanent control of positioning model geometry), and automatic alignment—lets users make the most of their measurement equipment and generate significant productivity gains without requiring extremely costly equipment or, most importantly, measurement environments.

Automatic alignment—and more broadly the automatic point measurement capabilities that optical CMMs already provide—is paving the way for the automation of optical measurement. Optical CMMs can already measure object deformation and movement in real time (dynamic tracking). Even though targets are still required, the scope for advancement in optics is enormous, as the rapid development of optical scanners has shown. Clearly, the future of 3D optical measurement has only just begun.

## Bibliography

- [1] American Society of Mechanical Engineers, ASME B89.4.22-2004 Method for Performance Evaluation of Articulated Arm Coordinate Measuring Machine, ASME, 2005.
- [2] International Organization for Standardization, ISO 2631-2:2003 Mechanical vibration and shock -- Evaluation of human exposure to whole-body vibration -- Part 2: Vibration in buildings (1 Hz to 80 Hz), ISO, 2003.
- [3] American National Standards Institute, ANSI s2.71-1983 (r2006) (formerly ANSI s3.29-1983) Guide to the Evaluation of Human Exposure to Vibration in Buildings, ANSI, 2006.
- [4] Australian Government - Department of Environment and Conservation, "Assessing vibrations: a technical guideline," 2006.
- [5] O. Hunaidi, "Réhabilitation des infrastructures urbaines," Canadian National research Council, Montreal, 2000.
- [6] M. P. Sharif and B. C. Warner, "Prediction of ground vibration induced by operation of heavy machinery," in *IMAC XX A Conference and Exposition on Structural Dynamics, Conference Proceedings*, 2000.
- [7] P. Mistrot, P. Donati, and J. Galmiche, "Exposition Vibratoire des opérateurs à proximité des machines industrielles," 2nd quarter 1997.
- [8] K. Atkinson, *Close Range Photogrammetry and Machine Vision*, Whittles Publishing, 1996.
- [9] O. Faugeras, *Three-Dimensional Computer Vision*, MIT Press éd., MIT Press, 1993.
- [10] R. Hartley and A. Zisserman, *Multiple View Geometry in Computer Vision*, Cambridge University Press, 2004.
- [11] M. R. Shortis and T. A. Clarke, "A comparison of some techniques for the subpixel location of discrete target images," *Videometrics III*, vol. 2350, pp. 239–250, 1994.
- [12] M. R. Shortis, T. A. Clarke, and S. Robson, "Practical Testing of the Precision and Accuracy of Target Image Centring Algorithms," *Videometrics IV*, vol. 2598, pp. 65–76, 1995.
- [13] J. Otepka, "Precision Target Mensuration in Vision Metrology," Technische Universität Wien, Vienna, 2004.
- [14] R. I. Hartley and P. Sturm, "Triangulation," *Computer Vision and Image Understanding*, vol. 68, no. 12, pp.

146–157, November 1997.

- [15] B. K. P. Horn, “Closed-form solution of absolute orientation using unit quaternions,” *Journal of the Optical Society of America*, vol. 4, pp. 629–642, 1987.
- [16] D. Eggert, A. Lorusso, and R. Fisher, “Estimating 3-D rigid body transformations: a comparison of four major algorithms,” *Machine Vision and Applications*, vol. 9, pp. 272–290, 1997.
- [17] H. Karara, *Non-Tophographic Photogrammetry*, American Society for Photogrammetry and Remote Sensing, 1989.
- [18] Verein Deutscher Ingenieure, VDI/VDE 2634 part 1: Optical 3D measuring systems - Imaging systems with point-by-point probing, 2002.
- [19] K. Bevan and T. Toman, "How Behavior Impacts Your Measurement," in *CMSC 2011 Measurement Study Report*, 2011.
- [20] Creaform 3D, “Handyscan 3D scanners - Handheld3D scanners,” Creaform 3D, [online]. Available: <http://www.creaform3d.com/en/handyscan3d/produits/default.aspx>. [Accessed April 12, 2012].
- [21] Creaform 3D, “HandyPROBE - Portable coordinate measuring machine (CMM),” [online]. Available: <http://www.creaform3d.com/en/handyprobe/handyprobe.aspx>. [Accessed April 24, 2012].
- [22] Creaform3D, “MetraSCAN optical CMM scanner,” [online]. Available: <http://www.creaform3d.com/en/metrascan/default.aspx>. [Accessed April 24, 2012].
- [23] Creaform 3D, “MaxSHOT 3D Optical Coordinate Measuring System,” [online]. Available: <http://www.creaform3d.com/en/maxshot3d/default.aspx>. [Accessed April 24, 2012].